Iranian Journal of Basic Medical Sciences
ijbms.mums.ac.ir

Spreading depression induces age- and caspase-specific patterns of neuronal injury in the rat brain

Arezou Eshaghabadi Niasari [1#], NoorMohammad Meshkinkhood [1#], Hasan Hosseini Ravandi [1], Sayed Mostafa Modarres Mousavi [1], Fatemeh Alipour [1], Sven G. Meuth [2], Maryam Khaleghi Ghadiri [3], Ali Gorji [3, 4, 5*]

[1] Shefa Neuroscience Research Center, Khatam Alanbia Hospital, Tehran, Iran
[2] Department of Neurology, University of Münster, Münster, Germany
[3] Department of Neurosurgery, University of Münster, Münster, Germany
[4] Epilepsy Research Center, University of Münster, Münster, Germany
[5] Neuroscience Research Center, Mashhad University of Medical Sciences, Mashhad, Iran

ARTICLE INFO

Article type:
Original

Article history:
Received: Jun 26, 2026
Accepted: Nov 8, 2026

Keywords:
Developing brain
Neocortex
Neuroprotection
Programmed cell death
Subarachnoid hemorrhage

ABSTRACT

Objective(s): To determine whether repetitive spreading depression (SD) induces neuronal injury and caspase-related apoptotic changes and to compare these effects between juvenile and adult rats.

Materials and Methods: Repetitive SD was induced in the somatosensory cortex of juvenile and adult Wistar rats. Neuronal injury and apoptosis were assessed by histology and TUNEL staining, while caspases 3, 8, 9, and 12 were evaluated by immunohistochemistry and Western blotting in neocortical and hippocampal tissues.

Results: Repetitive SD induced greater neuronal injury and DNA fragmentation in juvenile than adult rats, as indicated by increased dark neuron formation and TUNEL-positive cells. Caspase immunoreactivity showed age- and region-specific changes, with greater caspase-related immunoreactivity in the hippocampal and neocortical tissues of juvenile rats. In contrast, Western blot analysis showed decreased caspase-8 and caspase-9 protein levels, highlighting differences between tissue immunoreactivity and total protein expression. Caspase-12 immunoreactivity and protein levels showed no significant differences between SD and sham groups in either age group.

Conclusion: Repetitive SD induces age-, region-, and caspase-specific patterns of neuronal injury and apoptosis, with the developing brain showing greater susceptibility. The differential caspase findings suggest complex regulation of apoptotic pathways following repetitive SD and warrant further mechanistic investigation.

▶ Please cite this article as:
Eshaghabadi Niasari A, Meshkinkhood NM, Hosseini Ravandi H, Modarres Mousavi SM, Alipour F, Meuth SG, Khaleghi Ghadiri M, Gorji A. Spreading depression induces age- and caspase-specific patterns of neuronal injury in the rat brain. Iran J Basic Med Sci 2027; 30:

Corrected Proof

Introduction

Spreading depression, or depolarization (SD), is a slow-moving direct-current wave characterized by sudden, near-complete depolarization of neurons and glial cells, leading to profound disruptions in ionic gradients, energy metabolism, and neurotransmitter balance (1, **2**). SD contributes to several acute and chronic brain disorders, including traumatic brain injury, cerebrovascular diseases, and epilepsy (3-5). In energy-compromised or developing neural tissue, SD exacerbates metabolic stress, excitotoxicity, and neuroinflammation, leading to neuronal injury and death (6-8). Although SD has traditionally been considered harmless in the healthy adult brain (9), accumulating evidence suggests that repeated SD can induce neuronal damage, particularly in the metabolically active or immature neuronal tissues (10-13).

Caspases are essential enzymes that orchestrate apoptosis and mediate cellular injury (14). Among them, caspase-1 plays a pivotal role in the inflammatory cascade, with its activity changing transiently after SD, suggesting dynamic involvement in modulating neuroinflammation through cell–type–specific pro- and anti-inflammatory mechanisms (15,16). In ischemic rat brains, SD exacerbates injury by increasing caspase-3–positive neurons in the neocortex and hippocampus, an effect alleviated by the endogenous anti-inflammatory compound dimethyltryptamine (17). Similarly, in hypoglycemic retinas, SD-induced neuronal loss can be prevented by inhibition of SD or caspase-3 activity (18). Caspase activation is a common feature in SD-related disorders, including stroke, epilepsy, and traumatic brain injury (19). Yet, whether repetitive SD directly triggers caspase-mediated apoptosis remains unclear, a critical question given that caspase inhibition has demonstrated

*__Corresponding author:__ Ali Gorji. Epilepsy Research Center University of Münster Münster, Germany. Tel: +49-251-83-55564, Email: gorjial@uni-muenster.de
#These authors contributed equally to this work

© 2027. This work is openly licensed via CC BY 4.0.
This is an Open Access article distributed under the terms of the Creative Commons Attribution License (https://creativecommons.org/licenses), which permits unrestricted use, distribution, and reproduction in any medium, provided the original work is properly cited.

neuroprotective potential in various brain pathologies (20). Moreover, Developmental differences in mitochondrial function, neuronal maturation, and cell-survival pathways may influence caspase activation and neuronal vulnerability, particularly under pathological conditions like traumatic brain injury (21, 22). Thus, juvenile and adult brains may exhibit distinct caspase-dependent apoptotic responses under pathophysiological conditions such as SD. In this study, we investigated the roles of caspases in mediating the effects of repetitive SD on neuronal injury and apoptosis in juvenile and adult rat brains, focusing on caspase-3 as the primary executioner and caspase-9 and caspase-8 as key signaling components of the intrinsic and extrinsic apoptotic pathways. Caspase-12, involved in endoplasmic reticulum stress–induced apoptosis (23), was also evaluated. Assessing their expression profiles provides insight into the mechanisms underlying SD-related neuronal damage.

Materials and Methods

Each rat was kept individually under controlled laboratory conditions, maintained on a 12-hr light/12-hr dark cycle with unrestricted access to water and food. All experimental procedures complied with institutional ethical standards and were approved by the Ethics Committee of the Shefa Neuroscience Center, Tehran, Iran. The study included two groups of male Wistar rats: juvenile rats (3–5 weeks old; n=30) and adult rats (9–13 weeks old; n=30). Within each age group, 18 animals were designated for histological analyses (dark-cell quantification, TUNEL assay, and immunohistochemistry after perfusion), and the remaining 12 were allocated to Western blot analysis of fresh tissue.

Operative procedures

Anesthesia was induced with isoflurane (4%) for surgical preparation and electrode placement, and subsequently maintained with chloral hydrate (350 mg/kg, IP) before SD induction, due to its minimal interference with SD (24). Local analgesia was provided by application of lidocaine (2%) at incision sites. Animals were continuously monitored to assess anesthetic depth throughout the procedure. Postoperative analgesia was administered using meloxicam for up to 48 hr. Once sufficient anesthetic depth was achieved, animals were secured in a stereotaxic frame (Stoelting Instruments, USA). Two silver recording electrodes were placed over the somatosensory neocortex (~2 mm apart) and secured with dental acrylic cement, with the reference electrode positioned near the nose. A circular craniotomy (2 mm diameter) was created above the cortical surface, approximately 2-3 mm from the recording electrode, to induce SD. A small piece of cotton saturated with 2 M KCl solution was briefly applied to the dura for 2 min. The procedure was performed regardless of electrophysiological changes in DC potential and repeated at 20-min intervals. Bioelectrical signals were recorded using a DC-coupled amplifier at a sampling rate of 1kHz, without high-pass filtering, to preserve the slow DC potential fluctuations associated with SD. SD was identified by the characteristic negative DC potential shift recorded from the somatosensory cortex, followed by recovery toward baseline. Recordings affected by animal movement, electrode displacement, electrical interference, or unstable baseline activity were excluded from analysis. Control animals were treated identically, except that Ringer's solution replaced KCl solution. Each rat underwent four SD induction sessions, separated by one-week intervals. Electrocorticographic recordings were obtained continuously for up to 60 min following each event to monitor cortical bioelectrical activity. After each recording session, the injection site was sealed using pre-sterilized silicone and tissue adhesive, and tetracycline was applied to the burr holes to minimize infection risk.

Evaluation of dark cells

To ensure deep anesthesia, rats were administered sodium pentobarbital before transcardially perfusing with saline, followed by 4% paraformaldehyde (PFA). Brains were then removed, fixed in PFA for about seven days at 4 °C, dehydrated through graded ethanol, and embedded in paraffin. Serial coronal sections (7 µm) were mounted on glass slides, and sections were randomly selected for toluidine blue staining. Quantification of dark cells in the hippocampus (CA1 as well as CA3 subfields), somatosensory neocortex (SCX), and entorhinal cortex (EC) was done using a light microscope (BX51WI; Olympus, Japan) equipped with a digital camera and a 100× objective. Dark cells were distinguished by their characteristic nuclear and nucleolar staining patterns, and at least three randomly chosen microscopic fields were analyzed per section.

Detection of DNA fragmentation by TUNEL assay

Apoptotic DNA fragmentation was evaluated using a TUNEL Assay Kit–HRP-DAB (Abcam, UK) following the manufacturer's protocol with minor modifications. Tissue sections were first rehydrated through graded alcohol washes and rinsed in 1× TBS (pH 7.4). Tissue samples were then incubated with proteinase K for 20 min and washed in TBS at room temperature (RT). To inhibit endogenous peroxidase activity, tissues were incubated with H_2O_2 (0.3%) in methanol for 5 min, followed by a TBS wash. Next, slides were equilibrated in terminal deoxynucleotidyl transferase (TdT) buffer for 30 min at RT, incubated with the labeling reaction mixture (1 µl of TdT enzyme was combined with 39 µl of TdT labeling buffer) for 90 min at RT, and rinsed again in TBS. The reaction was terminated by adding stop buffer for 5 min; the tissue sections were then washed with TBS and treated with blocking buffer for 10 min. A 25× conjugate solution was applied for 30 min at RT and then washed with TBS. Color development was performed using DAB substrate for 15 min, and slides were rinsed with distilled water. Finally, slides were counterstained with methyl green for one min. TUNEL-positive cells were quantified by counting labeled nuclei in representative microscopic fields, and findings were described as the percentage of positive cells per sample.

Immunohistochemistry (IHC)

Brain sections were mounted on glass slides and rehydrated through graded alcohol and xylene, followed by a 5-minute rinse in distilled water and a 20-min wash in PBST (99.5% phosphate-buffered saline (PBS), 0.5% Triton X-100). Antigen retrieval was performed by boiling the sections in citrate buffer at 95 °C for 10 min. After cooling to RT, slides were washed in PBS and blocked for 1 hr at RT in PBS containing 5% normal goat serum (NGS) and 1% bovine serum albumin (BSA). Sections were then

Corrected Proof

incubated overnight at 4 °C with primary antibodies against caspase-3 (1:100; Abcam, UK), caspase-8 (1:50; Abcam, UK), caspase-9 (1:50; Proteintech, Germany), or caspase-12 (1:50; Abcam, UK) diluted in PBS with 5% NGS and 1% BSA. After three washes in TBST (0.9% NaCl, 0.06% Tris base, 0.05% Tween-20, pH 7.4), slides were incubated for 1 hr with FITC-conjugated anti-rabbit/mouse secondary antibodies (1:600; Abcam, UK) prepared in PBS with 5% NGS and 1% BSA. Cell nuclei were stained using propidium iodide. The sections were then mounted in 90% glycerol. Fluorescence images were captured using an Olympus BX51WI microscope equipped with a digital camera. Primary antibodies were omitted and replaced with normal goat serum as a negative control. Caspase-positive cells were quantified in 4 areas of every section, including the hippocampal CA1 and CA3 subfields, SCX, and EC, in both sham and SD-treated rats.

Western blotting

Tissue samples were rinsed in PBS, lysed with lysis buffer (ProteoJET Mammalian Cell Lysis Reagent, protease inhibitor), and centrifuged (15 min at 4 °C). Total protein concentration in the supernatant was determined using the conventional Bradford method. After one hour of electrophoresis in a 12.5% polyacrylamide gel, proteins were electrophoretically transferred from the gel onto a PVDF (polyvinylidene fluoride) membrane by a semi-dry western blotting system. The membranes were blocked with 2% ECL Prime Blocking Reagent, then incubated overnight at 4 °C with primary antibodies against β-Actin, cleaved caspase-3, and full-length caspase-8, -9, and -12 in blocking solution under continuous shaking. The membranes were rinsed in TBST containing 0.1% Tween 20 and incubated with horseradish peroxidase (HRP) secondary antibodies. Lastly, PVDF membranes were treated with cobalt chloride, imidazole, and 3,3′-diaminobenzidine substrate solution to detect the secondary antibody (25). Quantification of results was performed using GelAnalyzer 2010a software.

Statistical analysis

The data were analyzed using Prism 9 (GraphPad Software, USA). Differences among groups were evaluated using a two-way ANOVA, followed by Sidak's *post hoc* multiple-comparisons test. Values are presented as mean±SEM (standard error of the mean). A *P*-value<0.05 indicated statistical significance. The potential for limited statistical power in individual regional comparisons was acknowledged as a limitation and should be considered when interpreting the results.

Results

Induction of SD

Topical application of KCl to the SCX initiated SD, characterized by an initial negative direct current (DC) fluctuation followed by a positive deflection. In some recordings, a small transient positive deflection was observed immediately before the characteristic negative DC shift (26). This characteristic electrophysiological event was consistently observed across all recording sessions. During the first KCl application, SD had a mean amplitude of 8.4±0.3 mV and a duration of 90±3.7 sec. In the second to fourth weeks, SD amplitudes were 8.1±0.2, 8.4±0.4, and 8.2±0.3 mV, respectively, while durations were 85.5±3.1, 87.7±2.8, and 85.0±3.2 sec. No statistically significant differences were observed in SD amplitude or duration among the four weeks (*P*=0.8).

Dark cell formation and TUNEL assay after SD

Quantitative analysis revealed an increase in the number of dark cells within the CA3 and CA1 hippocampal subfields, EC, and SCX of juvenile SD rats versus the sham group (*P*<0.001; Figure 1). In adult animals, no significant differences were detected in the CA3 and CA1 subfields; however, SD-treated rats exhibited significantly greater dark neuron counts in both the EC (*P*<0.05) and SCX (*P*<0.01) versus the adult sham animals. Juvenile rats exposed to repetitive SD exhibited a significantly higher number of dark neurons in the CA3 (*P*<0.05) and CA1 (*P*<0.001) hippocampal regions compared to adult SD rats (Figure 1).

Analysis of TUNEL-labeled cells in the CA3 and CA1 subfields, EC, and SCX revealed a significant increase in TUNEL-positive cells in CA1 (*P*<0.05), CA3, EC, and SCX (*P*<0.001) in juvenile rats exposed to SD compared with controls (Figure 2). In contrast, SD induction in adult animals did not significantly alter TUNEL-positive cell counts across the examined brain regions compared with the sham groups.

Evaluation of caspase expression

A significant enhancement in caspase-3 reactivity was detected in the CA1 (*P*<0.01) and CA3 (*P*<0.05) subfields, EC, and SCX (*P*<0.05) areas of juvenile SD animals relative

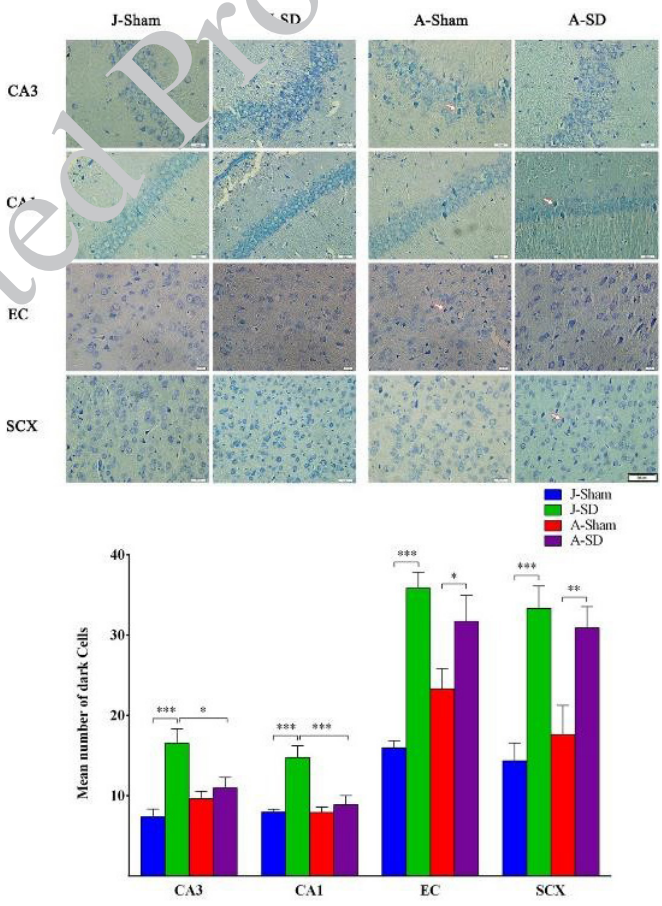


Figure 1. Repetitive spreading depression (SD) increases dark neuron formation in adult and juvenile rat brains

Representative toluidine blue–stained sections of the hippocampal CA3 and CA1 subfields, somatosensory neocortex (SCX), and entorhinal cortex (EC) from various groups of SD and sham-operated animals. Quantitative analyses of dark neuron counts across the examined brain regions in various groups are presented. Values are shown as mean±SEM. *, **, and *** indicate *P*<0.05, *P*<0.01, and *P*<0.001, respectively.

Corrected Proof

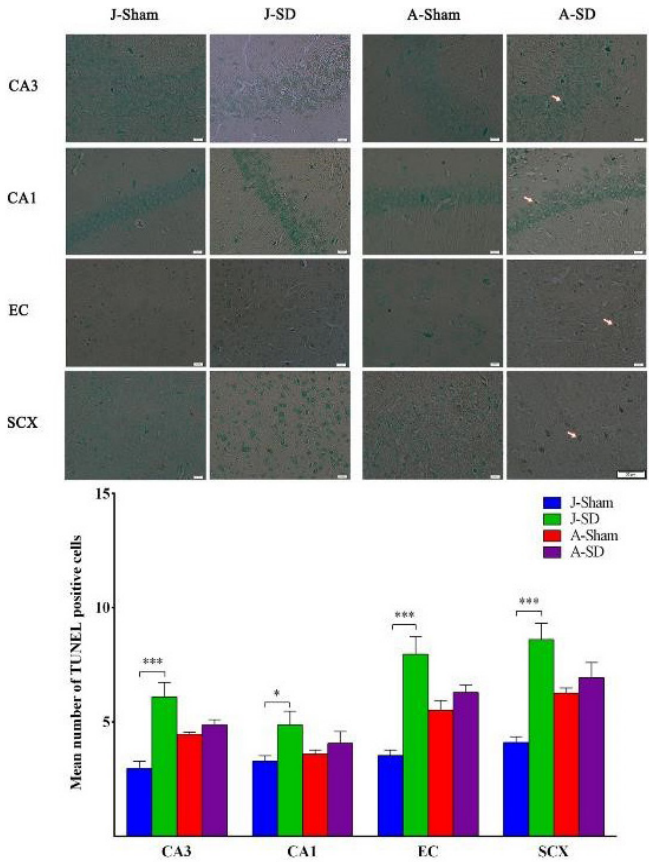


Figure 2. Repetitive SD increases TUNEL-positive cells in juvenile rat brains
Representative TUNEL-stained sections of the CA3 and CA1 subfields, SCX, and EC show more TUNEL-positive cells in SD-treated juvenile rats compared with sham controls. Bar graphs depict mean±SEM of TUNEL-positive cell counts across various brain regions. * $P<0.05$ and *** $P<0.001$.
SD: spreading depression; SCX: somatosensory neocortex; EC: entorhinal cortex

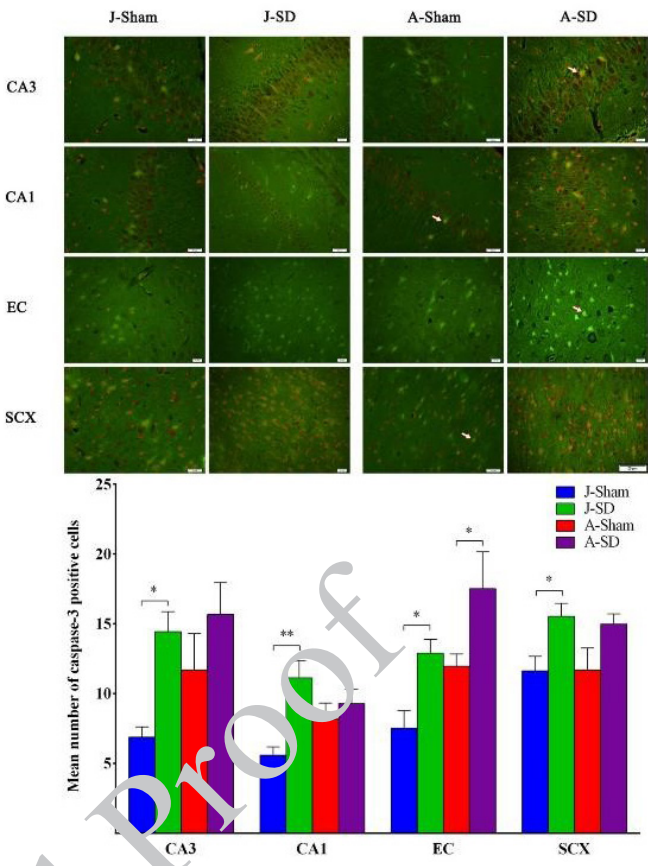


Figure 3. Repetitive SD increases caspase-3 expression in adult and juvenile rat brains
Representative immunofluorescence micrographs showing caspase-3 labeling in the CA3 and CA1 subfields, SCX, and EC of various groups of SD and sham-operated animals. Quantitative analysis of caspase-3–positive cells across the examined brain regions. Values are shown as mean±SEM. * $P<0.05$ and ** $P<0.01$.
SD: spreading depression; SCX: somatosensory neocortex; EC: entorhinal cortex

to controls. In contrast, adult SD-treated rats showed a significant elevation of caspase-3 expression only in the EC relative to control rats ($P<0.05$; Figure 3). Furthermore, juvenile rats exposed to SD showed greater caspase-8 immunoactivity in CA1 ($P<0.05$) and CA3 ($P<0.01$), as well as in EC ($P<0.01$) and SCX ($P<0.05$), than in controls. Moreover, caspase-8 expression in the EC was markedly greater in juvenile animals exposed to repetitive SD compared with adult SD-treated rats ($P<0.001$; Figure 4). Adult SD rats showed a non-significant trend toward increased caspase-8 expression in the SCX compared with adult controls ($P=0.06$; Figure 4), and caspase-8 levels did not change significantly in other examined regions (Figure 4).

Caspase-9 expression was also significantly up-regulated in juvenile SD rats, with increases in CA3 and CA1 ($P<0.05$) and in EC ($P<0.001$) and SCX ($P<0.01$) relative to controls. Expression of caspase-9 in the EC was significantly greater in juvenile animals subjected to repetitive SD than in adult SD animals ($P<0.001$; Figure 5). No significant alterations in caspase-9 immunoreactivity were detected in sham and SD-treated adult animals across the tested regions (Figure 5). In contrast, analysis of caspase-12 revealed no significant differences between SD and sham groups in either juvenile or adult rats across all examined regions (Figure 6). Juvenile SD rats showed a non-significant trend toward higher caspase-12 expression in CA3 and EC than juvenile shams ($P=0.09$; Figure 6), while adult SD rats showed a similar trend in the EC compared with adult controls ($P=0.08$; Figure 6).

Western blot assessment of caspase protein levels

Greater levels of cleaved caspase-3 expression were observed in both the neocortex ($P<0.05$) and hippocampus ($P<0.001$) of juvenile SD rats versus controls (Figures 7A–B and 8A–B). In adults, however, caspase-3 protein levels did not differ between SD and sham groups. In the neocortex, the values of caspase-8 were significantly reduced in juveniles but increased in adults following SD relative to age-matched control rats ($P<0.05$; Figure 7A, C). However, there were no significant differences in caspase-8 protein values in the hippocampus across groups (Figure 8A and C). Furthermore, SD induced a significant reduction of both neocortical and hippocampal caspase-9 values in juvenile rats relative to control rats ($P<0.01$; Figures 7 and 8A, D). A similar trend was observed in adults, where caspase-9 expression was likewise decreased in the hippocampus ($P<0.001$) and neocortex ($P<0.01$) relative to controls (Figures 7 and 8A, D). By contrast, caspase-12 protein levels remained unchanged across both age groups, with no significant alterations detected in the hippocampus or neocortex under SD versus sham conditions (Figures 7A

Corrected Proof

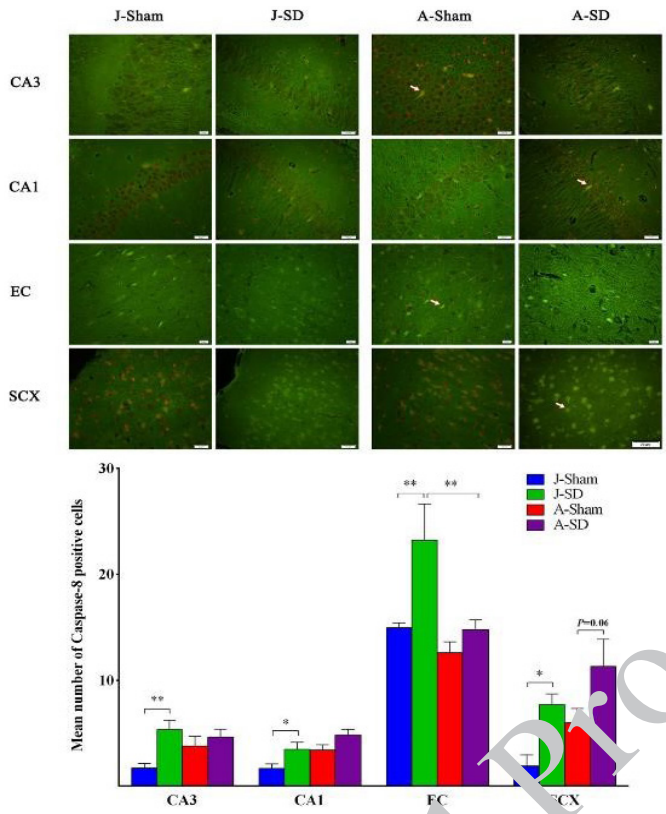


Figure 4. Repetitive SD enhances caspase-8 expression in juvenile rat brains
Representative immunofluorescence micrographs showing caspase-8 labeling in the CA3 and CA1 subfields, SCX, and EC from SD and sham-operated groups. Quantitative analysis of caspase-8–positive cells across the examined brain regions. Values are shown as mean±SEM. $P<0.05$ and ** $P<0.01$.
SD: spreading depression; SCX: somatosensory neocortex; EC: entorhinal cortex

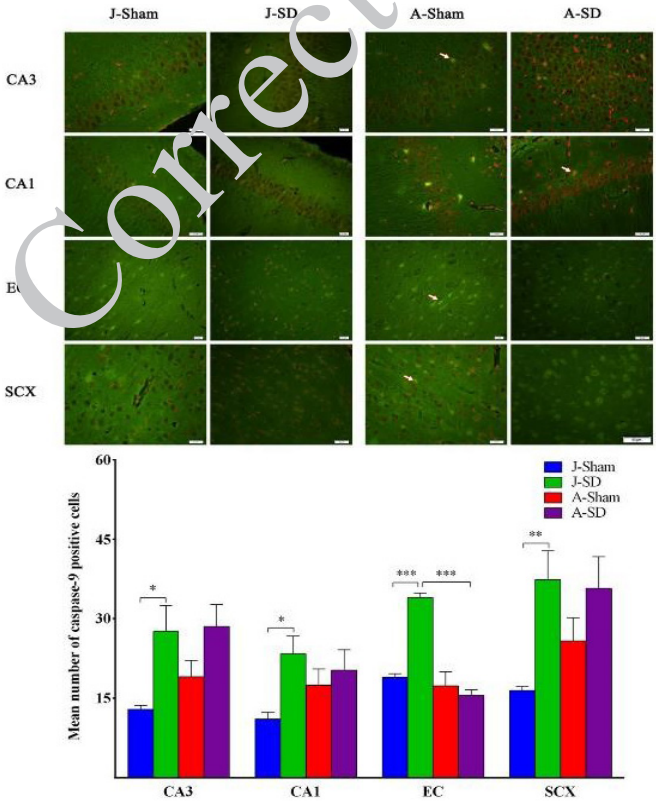


Figure 5. Repetitive SD increases caspase-9 expression in juvenile rat brains
Representative immunofluorescence micrographs showing caspase-9 labeling in the CA3 and CA1 subfields, SCX, and EC of various groups of SD and sham-operated rats. Quantitative analysis of caspase-9–positive cells across the various assessed brain regions. Bar graphs illustrate mean±SEM. * $P<0.05$, ** $P<0.01$, and *** $P<0.001$.
SD: spreading depression; SCX: somatosensory neocortex; EC: entorhinal cortex

Corrected Proof

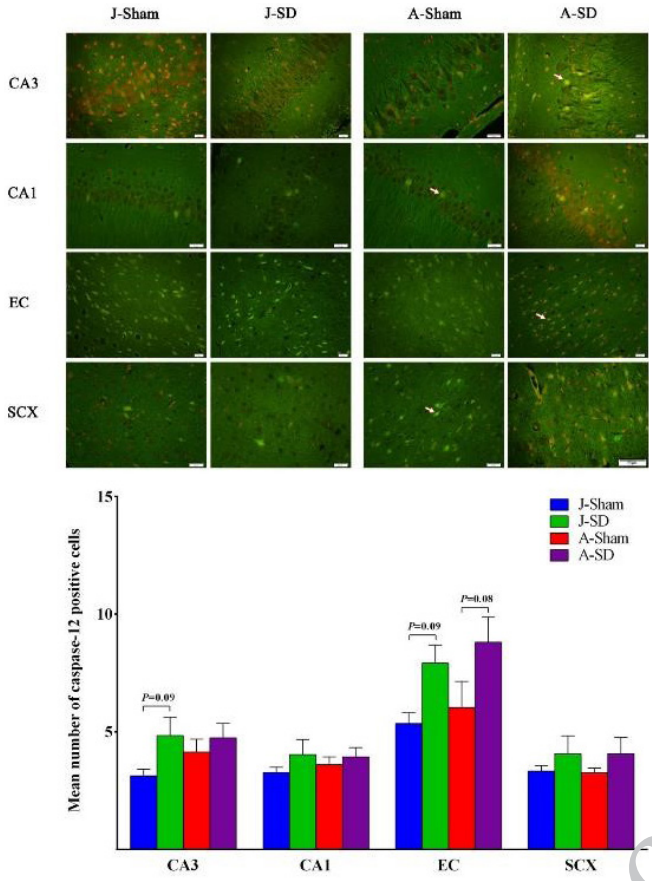


Figure 6. Caspase-12 Expression following SD in adult and juvenile rat brains
Representative immunofluorescence micrographs of caspase-12–positive cells in the CA3 and CA1 subfields, SCX, and EC of SD and sham-operated animals. Quantitative analysis of caspase-12–positive cells across the various assessed brain regions. Although no significant differences were observed between groups, expression trended higher in the juvenile SD group in the CA3 region and in both juvenile and adult SD groups in the EC. Values are shown as mean±SEM
SD: spreading depression; SCX: somatosensory neocortex; EC: entorhinal cortex

and E and 8A and E).

Discussion

Under normoxic conditions, our findings showed that the juvenile rat brain is more vulnerable to SD-induced injury than the adult brain, with both showing distinct region- and caspase-specific response patterns. In juvenile rats, SD induced marked neuronal injury, as evidenced by increased dark neuron formation, elevated TUNEL-positive cell numbers, and differential alterations in caspase-3, -8, and -9 expression. In contrast, adult rats subjected to SD exhibited less neuronal injury, with subtle changes in caspase expression, primarily confined to cortical regions.

Although an early study reported no clear evidence of cell injury in healthy conditions following repetitive SD induced within a single session and assessed a few days later (9), subsequent studies have demonstrated that SD can cause cellular injury in various areas of the nervous system, including the neocortex, hippocampus, and retina. Juvenile hippocampal slice cultures maintained under normoxic conditions revealed that repetitive SD events led to loss of field potentials, increased membrane depolarization, and marked neuronal damage, particularly in the hippocampal CA1 and CA3 subfields (11). In the chicken retina, repetitive SD produces progressively enlarging, irreversible macular lesions associated with elevated levels of cleaved caspase-3. Blocking SDs or inhibiting caspase activation prevents this damage, linking SD-driven energy failure to caspase-dependent cell death (17). Studies in juvenile rats also show that repetitive SD induces significant neuronal injury, characterized by increased dark and apoptotic neurons, reduced neuronal volume, and elevated expression of NR2B and GluR1 receptor subunits, indicating excitotoxic damage (12, 13). Moreover, in healthy mouse brains, multiple SDs trigger widespread transcriptional changes involving both injury-related and adaptive responses. While SD induces genes linked to metabolic stress and neuronal damage, it

Corrected Proof

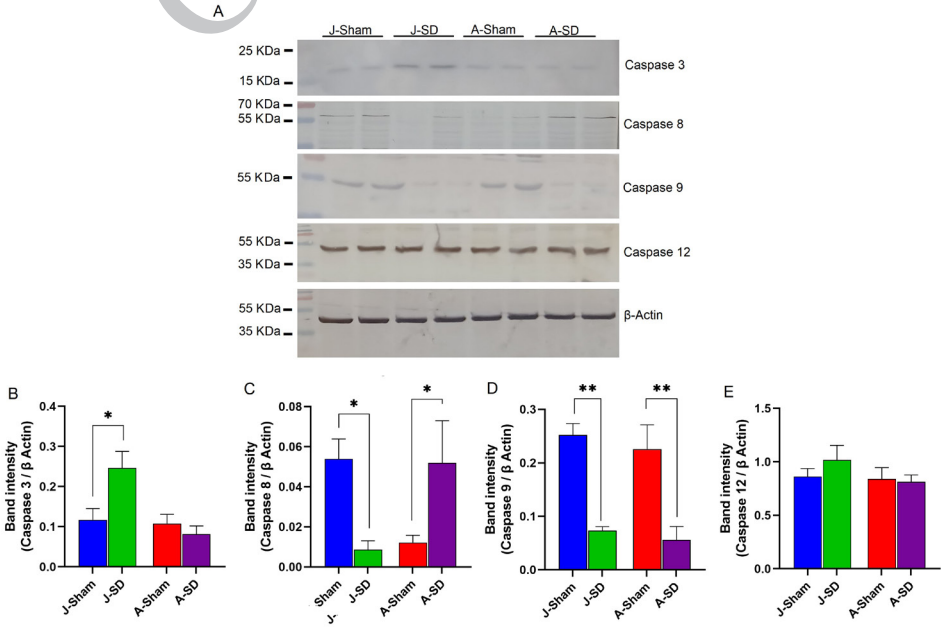


Figure 7. Impacts of repetitive SD on neocortical caspase-3, -8, -9, and -12 protein levels in adult and juvenile rat brains
(A) Representative Western blot images for each caspase are presented in various experimental groups. Band intensities of neocortical caspase-3 (B), caspase-8 (C), caspase-9 (D), and caspase-12 (E) were quantified and expressed relative to β-actin. Values are shown as mean±SEM. * $P<0.05$ and ** $P<0.01$.
SD: spreading depression

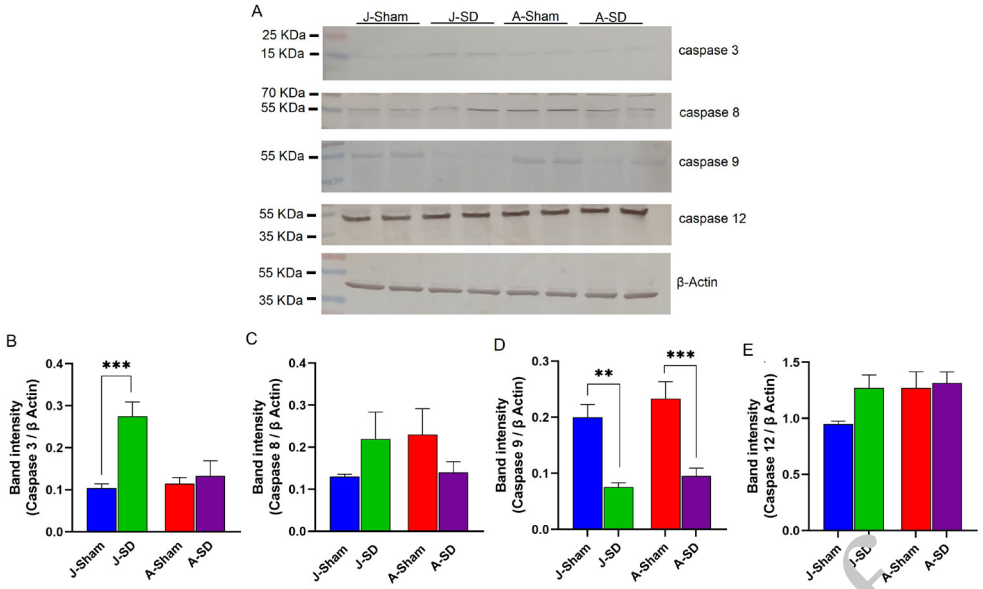


Figure 8. Impacts of repetitive SD on hippocampal caspase-3, -8, -9, and -12 protein levels in adult and juvenile rat brain. (A) Representative Western blots for each caspase are shown, illustrating the protein expression patterns in the sham and SD groups. Band intensities for hippocampal caspase-3 (B), caspase-8 (C), caspase-9 (D), and caspase-12 (E) were quantified and adjusted to β-actin. Values are shown as mean±SEM. $^{**}P<0.01$ and $^{***}P<0.001$.
SD: spreading depression

also activates pathways for synaptic plasticity, inflammation control, and neuroprotection (27).

The mechanisms underlying SD-induced neuronal injury involve a complex interplay between *(i)* mitochondrial dysfunction, *(ii)* neuroinflammatory signaling, and *(iii)* caspase-dependent apoptosis. Metabolic stress, ionic imbalance, and inflammation together increase cellular susceptibility to apoptosis, often mediated through caspase activation and calcium-dependent pathways (28). SD can initiate cellular stress responses, including calcium overload, mitochondrial impairment, and oxidative stress, each of which serves as a trigger for apoptosis (29,30). Mitochondrial alterations are central to this cascade. SD disrupts mitochondrial structure under normoxic conditions, causing dendritic mitochondria to fragment and swell, disorganizing the filamentous network, and producing dendritic beading in neurons (31, 32). Mitochondrial dysfunction results in the release of pro-apoptotic factors like cytochrome c, which in turn activates caspase-9 and enhances caspase-3–mediated apoptotic signaling (33, 34). This mechanism is especially relevant in neurons, where mitochondrial dysfunction increases susceptibility to apoptosis by promoting caspase-3 activation. Moreover, mitochondria may release intramitochondrial procaspase-3 during apoptosis, further enhancing executioner caspase protein levels (33-36). Concurrently, SD provokes neuroinflammatory responses. The expression of pro-inflammatory and apoptotic genes, including tumor necrosis factor, toll-like receptors, C-C motif chemokine ligand 2, cyclooxygenase-2, interleukins-6 and -1, and B-cell lymphoma 2, is significantly increased in response to SD (8, 37, 38). SD activates neuronal Panx1 channels, which in turn stimulate the inflammasome, leading to caspase-1 activation and the ensuing release of interleukin-1β and high mobility group box 1 protein, thus initiating neuroinflammation (39). Caspase-1 activation can indirectly promote apoptosis by inducing mitochondrial dysfunction, generating reactive oxygen species, triggering cytokine-mediated signaling, and depleting energy, thereby leading to secondary apoptotic cell death, particularly under metabolic stress (40). Our IHC results showed that SD markedly increased caspase-8, -9, and -3 immunoreactivity in the juvenile rat brain, indicating activation and cross-talk between the extrinsic and intrinsic apoptotic pathways, with caspase-3 confirming apoptotic execution (41). Caspase-9 protein levels were reduced in both juvenile and adult brains after SD; however, because cleaved caspase-9 was not directly assessed, these findings cannot be interpreted as evidence of caspase-9 activation and may reflect altered regulation of the intrinsic apoptotic pathway.

Although caspases-3, -8, and -9 showed significant alterations, caspase-12 expression was not significantly affected by SD in either IHC or Western blot analyses. However, IHC revealed modest trends toward increased expression in the CA3 and EC regions. This pattern suggests that SD-related apoptosis may involve pathways other than the caspase-12-associated endoplasmic reticulum (ER) stress pathway (42). Consistent with this possibility, OGD/R-induced neuronal injury has been shown to activate caspases-3, -8, and -9 without significant caspase-12 cleavage, despite evidence of ER stress (43). This study suggests that ER stress may activate caspase-8/-9-mediated apoptosis through a BiP–CHOP pathway independently of caspase-12, suggesting a potential caspase-12-independent mechanism in SD that warrants further investigation. During the juvenile stage, the brain undergoes rapid structural and functional maturation, marked by intense neuronal growth, peak synaptogenesis, glial activation, and blood–brain barrier remodeling, making it inherently more vulnerable to injury due to increased sensitivity to mitochondrial dysfunction and neuroinflammation (44, 45). Previous studies indicate that the immature brain is more susceptible to oxidative stress and mitochondrial dysfunction because of underdeveloped antioxidant defenses, less efficient mitochondrial function, and higher metabolic demand (46, 47). A key distinction between immature and mature

Corrected Proof

brain tissue is that adult neurons can tolerate longer periods of membrane depolarization and elevated intracellular calcium than immature neurons (48, 49). Neurons that remain depolarized for an extended period following SD are susceptible to calcium-dependent damage (50, 51). In the immature brain, where neurovascular coupling and energy reserves are limited, these factors are particularly harmful to vulnerable tissues, potentially enhancing neuronal stress and increasing susceptibility to cell injury and apoptosis (50, 51, 52). Increased caspase-3 activity is a hallmark of the immature brain, contributing to its heightened vulnerability to injury (53). Caspase-3 activation in response to neuronal injury is significantly higher in juvenile rats than in adults, indicating a greater reliance of immature neurons on caspase-mediated apoptosis (54). The high levels of caspase-3 observed in the immature brain suggest enhanced apoptotic activity relative to the adult brain (55, 56).

Targeting caspase protein levels has been suggested as a potential therapeutic strategy for SD-related neurological disorders, including epilepsy (19, 57), cerebrovascular diseases (58, 59), and traumatic brain injury (60-62). Recent strategies to inhibit SD have increasingly focused on targeting glutamate sub-receptors and other ion channels, aiming to minimize the sustained neuronal damage that can persist well beyond the initiating insult (63). Our findings revealed that SD triggers activation of both initiator and executioner caspases, leading to neuronal damage in hippocampal and cortical regions, particularly in the immature brain. This provides mechanistic insight and suggests the potential for targeting caspase signaling in SD-related neurological disorders.

Alterations in caspase signaling have been implicated in neurological disorders associated with SD, including epilepsy (19, 57, 58), cerebrovascular diseases (59, 60), and traumatic brain injury (61-63). However, the therapeutic relevance of caspase modulation in SD remains to be established. Recent approaches to limiting SD-related injury have increasingly focused on glutamate receptors and ion channels to reduce sustained neuronal stress and damage that may persist beyond the initiating insult (64). In the present study, SD was associated with altered protein expression of caspases-3, -8, and -9 across hippocampal and neocortical regions, with more pronounced changes observed in the immature brain. Further studies using pathway-specific inhibitors and direct assessment of cleaved caspases will be required to determine whether modulation of these pathways can reduce SD-related neuronal injury.

A limitation of our study is that it included only male rats. This was intentional because ovarian hormones, particularly estrogen and progesterone, can modulate SD characteristics (65) and neuronal apoptotic signaling, including caspase-3 expression and activation, potentially introducing hormonal variability (66). However, this limits the generalizability of our findings to females and warrants future investigation of sex- and hormone-dependent differences. Another limitation is our use of focal KCl application as an established, reproducible model of SD, which may not fully recapitulate the complex pathophysiological conditions of SD in neurological disorders. Moreover, the absence of functional or behavioral outcomes limits conclusions regarding neurological consequences. Finally, caspase alterations were correlative and do not establish a causal role for specific caspases in SD-induced neuronal injury. Future studies using selective caspase inhibition, genetic manipulation, or pathway-specific interventions are needed to determine the causal contribution and therapeutic potential of caspase signaling, particularly during brain development.

Conclusion

Our findings suggest that SD-induced neuronal injury under normoxic conditions is age-dependent, with the immature brain exhibiting greater vulnerability than the adult brain. The observed changes in caspase-3, -8, and -9 expression indicate the involvement of apoptotic signaling pathways in SD-related neuronal injury. These results point to the importance of age-dependent susceptibility to SD-induced neuronal injury and highlight the need for further studies to elucidate the underlying mechanisms and identify potential therapeutic strategies.

Acknowledgment

None.

Data Availability

The data supporting the findings of this study are available from the corresponding author upon reasonable request.

Funding

None

Authors' Contributions

A EN, N M, and H HR performed the experiments. H HR, F A, and N M prepared the figures. A EN, SM MM, and FA analyzed the data; F A also conducted the statistical analysis. SG M and M KG contributed to the study design and reviewed the manuscript. A G conceived, designed, and supervised the study and prepared the initial draft. All authors read and approved the final manuscript.

Conflicts of Interest

The authors have no conflicts of interest to declare

Declaration

We have not used AI tools or technologies to prepare this manuscript, except for language refinement.

References

1. Somjen GG. Mechanisms of spreading depression and hypoxic spreading depression-like depolarization. Physiol Rev 2001;81:1065–1096.
2. Chever O, Zerimech S, Scalmani P, Lemaire L, Pizzamiglio L, Loucif A, *et al.* Initiation of migraine-related cortical spreading depolarization by hyperactivity of GABAergic neurons and NaV1.1 channels. J Clin Invest 2021;131.
3. Hill A, Amendolara AB, Small C, Guzman SC, Pfister D, McFarland K, *et al.* Metabolic pathophysiology of cortical spreading depression: a review. Brain Sci 2024;14:1026.
4. Dreier JP. The role of spreading depression, spreading depolarization and spreading ischemia in neurological disease. Nat Med. 2011;17:439–447.
5. Kazemi H, Rahgozar M, Speckmann E, Gorji A. Effect of cannabinoid receptor activation on spreading depression. Iran J Basic Med Sci 2012;15:926–936.
6. Obeidat AS, Andrew RD. Spreading depression determines acute cellular damage in the hippocampal slice during oxygen/glucose deprivation. Eur J Neurosci 1998;10:3451–3461.
7. Hartings JA, Shuttleworth CW, Kirov SA, Ayata C, Hinzman JM, Foreman B, *et al.* The continuum of spreading depolarizations

Corrected Proof

in acute cortical lesion development: Examining Leão's legacy. J Cereb Blood Flow Metab 2017;37:1571–1594.
8. Ashayeri Ahmadabad R, Khaleghi Ghadiri M, Gorji A. The role of Toll-like receptor signaling pathways in cerebrovascular disorders: The impact of spreading depolarization. J Neuroinflammation. 2020;17:108.
9. Nedergaard M, Hansen AJ. Spreading depression is not associated with neuronal injury in the normal brain. Brain Res 1988;449:395–398.
10. MacLean MA, Muradov JH, Greene R, Van Hameren G, Clarke DB, Dreier JP, *et al*. Memantine inhibits cortical spreading depolarization and improves neurovascular function following repetitive traumatic brain injury. Sci Adv 2023;9.
11. Pomper JK, Haack S, Petzold GC, Buchheim K, Gabriel S, Hoffmann U, *et al*. Repetitive spreading depression-like events result in cell damage in juvenile hippocampal slice cultures maintained in normoxia. J Neurophysiol 2006;95:355–368.
12. Jafarian M, Rahimi S, Behnam F, Hosseini M, Haghir H, Sadeghzadeh B, *et al*. The effect of repetitive spreading depression on neuronal damage in juvenile rat brain. Neuroscience 2010;169:388–394.
13. Sadeghian H, Jafarian M, Karimzadeh F, Kafami L, Kazemi H, Coulon P, *et al*. Neuronal death by repetitive cortical spreading depression in juvenile rat brain. Exp Neurol 2012;233:438–446.
14. Aziz N, Hussain G, Abbas Q. Role of microRNAs in major brain diseases, focusing on neuroinflammation and neuronal apoptosis. Iran J Basic Med Sci.2026;29:844–869.
15. Chen PY, Yen JC, Liu TT, Chen ST, Wang SJ, Chen SP. Neuronal NLRP3 inflammasome mediates spreading depolarization-evoked trigeminovascular activation. Brain 2023;146:2989–3002.
16. Kaya Z, Belder N, Sever-Bahcekapili M, Erdener ŞE, Dönmez-Demir B, Bağcı C, *et al*. Spreading depolarization triggers pro- and anti-inflammatory signalling: a potential link to headache. Brain 2025;148:2522–2536.
17. Szabó Í, Varga VÉ, Dvorácskó S, Farkas AE, Körmöczi T, Berkecz R, *et al*. N,N-Dimethyltryptamine attenuates spreading depolarization and restrains neurodegeneration by sigma-1 receptor activation in the ischemic rat brain. Neuropharmacology 2021;192:108612.
18. Yu Y, Santos LM, Mattiace LA, Costa ML, Ferreira LC, Benabou K, *et al*. Reentrant spiral waves of spreading depolarization cause macular degeneration in hypoglycemic chicken retina. Proc Natl Acad Sci U S A 2012;109:2585–2589.
19. Zhang A, Zhang Z, Liu Y, Lenahan C, Xu H, Jiang J, *et al*. The role of caspase family in acute brain injury: The potential therapeutic targets in the future. Curr Neuropharmacol 2022;20:1194–1211.
20. Dhani S, Zhao Y, Zhivotovsky B. A long way to go: Caspase inhibitors in clinical use. Cell Death Dis 2021;12:949.
21. Yakovlev AG, Ota K, Wang G, Movsesyan V, Bao WL, Yoshihara K, *et al*. Differential expression of apoptotic protease-activating factor-1 and caspase-3 genes and susceptibility to apoptosis during brain development and after traumatic brain injury. J Neurosci 2001;21:7439–7446.
22. Bittigau P, Sifringer M, Pohl D, Stadthaus D, Ishimaru M, Shimizu H, *et al*. Apoptotic neurodegeneration following trauma is markedly enhanced in the immature brain. Ann Neurol 1999;45:724–735.
23. Sahoo G, Samal D, Khandayataray P, Murthy MK. A review on caspases: Key regulators of biological activities and apoptosis. Mol Neurobiol 2023;60:5805–5837.
24. Kudo C, Nozari A, Moskowitz MA, Ayata C. The impact of anesthetics and hyperoxia on cortical spreading depression. Exp Neurol 2008;212:201–206.
25. Pukac LA, Carter JE, Morrison KS, Karnovsky MJ. Enhancement of diaminobenzidine colorimetric signal in immunoblotting. Biotechniques 1997;23:385–388.
26. Kovac S, Speckmann EJ, Gorji A. Uncensored EEG: The role of DC potentials in neurobiology of the brain. Prog Neurobiol 2018;165–167:51–65.
27. Dell'Orco M, Weisend JE, Perrone-Bizzozero NI, Carlson AP, Morton RA, Linsenbardt DN, *et al*. Repetitive spreading depolarization induces gene expression changes related to synaptic plasticity and neuroprotective pathways. Front Cell Neurosci 2023;17:1292661.
28. Zong Y, Li H, Liao P, Chen L, Pan Y, Zheng Y, *et al*. Mitochondrial dysfunction: Mechanisms and advances in therapy. Signal Transduct Target Ther 2024;9:124.
29. Dietz RM, Weiss JH, Shuttleworth CW. Contributions of Ca^{2+} and Zn^{2+} to spreading depression-like events and neuronal injury. J Neurochem 2009;109:145–152.
30. Soylu KO, Yemisci M, Karatas H. The link between spreading depolarization and innate immunity in the central nervous system. J Headache Pain 2025;26:25.
31. van Hameren G, Muradov J, Minarik A, Aboghazleh R, Orr S, Cort S, *et al*. Mitochondrial dysfunction underlies impaired neurovascular coupling following traumatic brain injury. Neurobiol Dis 2023;186:106269.
32. Sword J, Fomitcheva IV, Kirov SA. Spreading depolarization causes reversible neuronal mitochondria fragmentation and swelling in healthy, normally perfused neocortex. J Cereb Blood Flow Metab 2024;44:1561–1579.
33. Green DR, Reed JC. Mitochondria and apoptosis. Science 1998;281:1309–1312.
34. Adrain C, Martin SJ. The mitochondrial apoptosome: A killer unleashed by the cytochrome seas. Trends Biochem Sci 2001;26:390–397.
35. Mancini M, Nicholson DW, Roy S, Thornberry NA, Peterson EP, Casciola-Rosen LA, *et al*. The caspase-3 precursor has a cytosolic and mitochondrial distribution: Implications for apoptotic signaling. J Cell Biol 1998;140:1485–1495.
36. Kuida K, Zheng TS, Na S, Kuan C, Yang D, Karasuyama H, *et al*. Decreased apoptosis in the brain and premature lethality in CPP32-deficient mice. Nature 1996;384:368–372.
37. Gunder S, Schroeter M, Peters O, Witte OW, Stoll G. Cortical spreading depression induces proinflammatory cytokine gene expression in the rat brain. J Cereb Blood Flow Metab 2001;21:218–225.
38. Takizawa T, Qin T, Lopes de Morais A, Sugimoto K, Chung JY, Morsett L, *et al*. Non-invasively triggered spreading depolarizations induce a rapid pro-inflammatory response in cerebral cortex. J Cereb Blood Flow Metab 2020;40:1117–1131.
39. Karatas H, Erdener SE, Gursoy-Ozdemir Y, Lule S, Eren-Koçak E, Sen ZD, *et al*. Spreading depression triggers headache by activating neuronal Panx1 channels. Science 2013;339:1092–1095.
40. Guo H, Pétrin D, Zhang Y, Bergeron C, Goodyer CG, LeBlanc AC. Caspase-1 activation of caspase-6 in human apoptotic neurons. Cell Death Differ 2006;13:285–292.
41. Dho SH, Cho M, Woo W, Jeong S, Kim LK. Caspases as master regulators of programmed cell death: Apoptosis, pyroptosis and beyond. Exp Mol Med 2025;57:1121–1132.
42. Alipour F, Modarres Mousavi SM, Nourbaksh F, Ghadipasha M, Gharehdaghi J, Kellinghaus C, *et al*. Apoptosis and glial marker profiles in hippocampus and amygdala of medically intractable temporal lobe epilepsy. J Cell Mol Med 2026;30:e71179.
43. Tian Y, Wang L, Qiu Z, Xu Y, Hua R. Autophagy triggers endoplasmic reticulum stress and C/EBP homologous protein-mediated apoptosis in OGD/R-treated neurons in a caspase-12-independent manner. J Neurophysiol 2021;126:1740–1750.
44. Zhao S, Wang X, Gao X, Chen J. Delayed and progressive damages to juvenile mice after moderate traumatic brain injury. Sci Rep 2018;8:7339.
45. Hagberg H, Mallard C, Rousset CI, Thornton C. Mitochondria: Hub of injury responses in the developing brain. Lancet Neurol 2014;13:217–232.
46. Jiang Q, Wen J, Ding Y, Cui H. From vulnerability to resilience: Unraveling the role of oxidative stress in preterm brain injury. Ital J Pediatr 2025;51:232.
47. Blomgren K, Hagberg H. Free radicals, mitochondria, and hypoxia-ischemia in the developing brain. Free Radic Biol Med 2006;40:388–397.

Corrected Proof

48. Gainutdinov A, Juzekaeva E, Mukhtarov M, Khazipov R. Anoxic spreading depolarization in the neonatal rat cortex *in vitro*. Front Cell Neurosci 2023;17:1106268.
49. Somjen GG. Is spreading depression bad for you? Focus on „repetitive normoxic spreading depression-like events result in cell damage in juvenile hippocampal slice cultures". J Neurophysiol 2006;95:16–17.
50. Herreras O, Somjen GG. Effects of prolonged elevation of potassium on hippocampus of anesthetized rats. Brain Res 1993;617:194–204.
51. Pensato U, Ospel J, Lemale CL, Hartings J, Romoli M, Sacco S, *et al*. Spreading depolarization: A wave that precedes and drives cerebral ischemic cell death—target for neuroprotection. J Cereb Blood Flow Metab 2026;46:1759–1781.
52. Mayevsky A, Zarchin N, Friedli CM. Factors affecting the oxygen balance in the awake cerebral cortex exposed to spreading depression. Brain Res 1982;236:93–105.
53. Johnston MV, Fatemi A, Wilson MA, Northington F. Treatment advances in neonatal neuroprotection and neurointensive care. Lancet Neurol 2011;10:372–382.
54. Hu BR, Liu CL, Ouyang Y, Blomgren K, Siesjö BK. Involvement of caspase-3 in cell death after hypoxia-ischemia declines during brain maturation. J Cereb Blood Flow Metab 2000;20:1294–1300.
55. Thornton C, Hagberg H. Role of mitochondria in apoptotic and necroptotic cell death in the developing brain. Clin Chim Acta 2015;451:35–38.
56. Thornton C, Leaw B, Mallard C, Nair S, Jinnai M, Hagberg H. Cell death in the developing brain after hypoxia-ischemia. Front Cell Neurosci 2017;11:248.
57. Bassil F, Fernagut PO, Bezard E, Pruvost A, Leste-Lasserre T, Hoang QQ, *et al*. Reducing C-terminal truncation mitigates synucleinopathy and neurodegeneration in a transgenic model of multiple system atrophy. Proc Natl Acad Sci U S A 2016;113:9593–58. Jafarian M, Modarres Mousavi SM, Alipour F, Aligholi H, Noorbakhsh F, Ghadipasha M, *et al*. Cell injury and receptor expression in the epileptic human amygdala. Neurobiol Dis 2019;124:416–427.
59. Pei X, Tian M, Wang Y, Xin Y, Jiang J, Wang Y, *et al*. Advances in the knowledge on the role of apoptosis repressor with caspase recruitment domain in hemorrhagic stroke. J Intensive Med 2023;3:138–143.
60. Wang C, Huang Y, Gong Y, Wu M, Jiang L, Dang B. Tetramethylpyrazine protects mitochondrial function by up-regulation of TFAM and inhibition of neuronal apoptosis in a rat model of surgical brain injury. Iran J Basic Med Sci 2024;27:352–359.
61. Legos JJ, Lee D, Erhardt JA. Caspase inhibitors as neuroprotective agents. Expert Opin Emerg Drugs 2001;6:81–94.
62. Unnisa A, Greig NH, Kamal MA. Inhibition of caspase 3 and caspase 9 mediated apoptosis: a multimodal therapeutic target in traumatic brain injury. Curr Neuropharmacol 2023;21:1001–1012.
63. Li B, Zhou Y, Yang G, Li B, Zhu M, Lu D, *et al*. Voluntary exercise alleviates ischemic brain injury in mice by modulating mitochondrial dysfunction. Iran J Basic Med Sci 2025;28:846–851.
64. Kramer DR, Fujii T, Ohiorhenuan I, Liu CY. Cortical spreading depolarization: Pathophysiology, implications, and future directions. J Clin Neurosci 2016;24:22–27.
65. Sachs M, Pape HC, Speckmann EJ, Gorji A. The effect of estrogen and progesterone on spreading depression in rat neocortical tissues. Neurobiol Dis 2007;25:27–34.
66. Zhang B, Bruynani BR. Glutamate-induced apoptosis in primary cortical neurons is inhibited by equine estrogens via down-regulation of caspase-3 and prevention of mitochondrial cytochrome c release. BMC Neurosci 2005;6:13.

Corrected Proof